BUTTERWORTH HEINEMANN

Polymer Vol. 36 No. 21, pp. 4011–4021, 1995

0032-3861/95/$10.00 + 0.00

Vibrational and n.m.r. study of poly(*N*-methyllaurolactam) and of poly(*N*-methyllaurolactam)–poly(4-vinylphenol) blends

P. Schmidt, J. Straka*, J. Dybal, B. Schneider, D. Doskočilová and R. Puffr
Institute of Macromolecular Chemistry, Academy of Sciences of the Czech Republic, 162 06 Prague 6, Czech Republic
(Received 18 January 1995)

Poly(*N*-methyllaurolactam) (PNMLL) and its blends with poly(4-vinylphenol) (PVPh) were studied by a combination of infra-red, Raman and n.m.r. spectroscopic methods. In the crystalline phase of semicrystalline PNMLL, the amide bond was shown to be present in the *cis* form, and the polymethylene chain to contain long *trans* sequences, with a *trans* conformation on the $-CH_2-CO-$ bond. In the blends, the content of the crystalline phase, and also of the polymethylene *trans* sequences, is strongly suppressed. Analysis of the O–H stretching vibrations shows that in the blends the hydrogen bonds between the O–H groups of PVPh and PNMLL carbonyls are stronger than the hydrogen bonds in pure PVPh. The values of $T_{1\rho}^{H}$ relaxation times indicate intimate mixing of the blend components on a scale of <3 nm.

(Keywords: poly(*N*-methyllaurolactam); poly(4-vinylphenol); blends)

INTRODUCTION

In our previous studies we have used a combination of vibrational and n.m.r. spectroscopy for the investigation of the structure and dynamics of polymer blends with weak and medium intermolecular interactions between the components[1,2]. In this study, we have chosen a similar approach for the case of the blends of poly(*N*-methyllaurolactam) and poly(4-vinylphenol) (PNMLL/PVPh), where that interaction is strong.

Atactic amorphous poly(4-vinylphenol) (PVPh) can form hydrogen bonds by means of its hydroxy groups with all polymers containing carbonyl groups. It has often been used as one of the components in structural studies of blends with strong interactions, and its spectral behaviour is generally known[3–6].

Poly(*N*-methyllaurolactam) (PNMLL) is a semicrystalline polymer, with a T_g of ~−35°C. Its structure was studied many years ago by infra-red and low-field n.m.r. spectroscopy, and by X-ray and d.s.c. measurements[7]. Assuming the existence of the *cis* and *trans* structures of the *N*-methylated amide group, and considering infra-red band intensity ratios, the authors concluded that in the crystalline phase of PNMLL the methyl group assumes *trans* orientation with respect to the carbonyl oxygen.

In order to evaluate correctly the effects of blending, we have re-examined the structure of PNMLL by a combination of infra-red (i.r.), Raman, solution and solid-state n.m.r. spectra, and values of X-ray crystallinity, and used the same combination of methods for characterizing the structure of blends.

EXPERIMENTAL

Samples

Poly(*N*-methyllaurolactam) was prepared by acidolytic polymerization of *N*-methyllaurolactam[8], initiated with 0.66 mol% dodecanoic acid per mole of lactam, at 260°C for 72 h (polymer yield 99.2%), and also by cationic polymerization initiated with 0.55 mol% $AlCl_3$ per mole of lactam at 260°C for 2 h[9]. Poly(4-vinylphenol) (PVPh) with $M_w = 30\,000$ was obtained from Polyscience Inc. PNMLL/PVPh blends were prepared by separate dissolution of the polymers in tetrahydrofuran followed by mixing of the solutions and evaporation of the solvent. We have studied the PNMLL/PVPh blends at the component molar ratios 4:1, 1:1 and 1:4.

Measurements

Films for infra-red measurements were cast on KBr windows. For the preparation of oriented PNMLL, a film cast on a Teflon plate was fastened between two holders and slowly stretched and elongated by means of a screw[3,4]. Infra-red spectra were measured on Bruker IFS-55 and IFS-88 *FT*i.r. spectrometers and on a Perkin-Elmer 580B grating infra-red spectrometer connected on-line with a Tracor TN-4000 multichannel analyser. Low-temperature infra-red spectra were measured using an RIIC variable temperature cell. Infra-red dichroism of the oriented neck of the elongated PNMLL was

* To whom correspondence should be addressed

measured using an AgBr polarizer positioned in the sample compartment of the IFS-55.

For the measurement of Raman spectra the samples were used as prepared. Spectra were recorded at 2 cm^{-1} resolution on a Bruker IFS-55 *FT*i.r. spectrometer equipped with the Raman module FRA-106. The samples were excited by a 1064 nm diode-pumped Nd:YAG laser with a power of 200 mW at the sample.

Solid-state n.m.r. spectra were measured on a Bruker MSL 200 spectrometer at 50.3 MHz (^{13}C) using the standard combination of cross-polarization (CP), dipolar decoupling (DD) and magic-angle spinning (MAS)[10]. The MAS frequency was 4 kHz, the spectra were externally referenced to the signal of the carbonyl carbon of glycine ($\delta = 176.0$ ppm from TMS) by sample replacement. The rotating-frame spin-lattice relaxation time for protons, $T_{1\rho}^{H}$, was measured indirectly from the ^{13}C CP/MAS/DD n.m.r. spectra. The experimental scheme used a variable spin-lock time followed by constant contact time. The spectra of amorphous and crystalline components of PNMLL were separately measured based on assumed differences in T_1^C relaxation. The amorphous component of PNMLL was measured without CP by using 90°C pulses at 1 s intervals and the crystalline component was measured by the method for T_1^C measurements with cross polarization[11] using a delay of 10 s.

All high-resolution n.m.r. spectra were recorded on a Bruker ACF-300 spectrometer, at resonance frequencies of 300.1 for ^1H and 75.5 MHz for ^{13}C. The polymers were measured as ~10% wt/vol solutions in 1,1,2,2-tetrachloroethane-d_2 (TCE). For measurements at elevated temperatures the measuring cell was flushed with argon and sealed. All chemical shifts are referenced to internal hexamethyldisiloxane (HMDS, shifts δ with respect to TMS: 0.05 ppm for ^1H, 2 ppm for ^{13}C). The pulse angle was 30°, and the pulse interval was 2.7 s. ^1H–^1H COSY spectra[12] were measured at 300 MHz with 1024 points and 256 increments, with zero filling to 1024 points and 80 scans per increment. Sine bell weighting functions in both dimensions were used before Fourier transformation, and a symmetrization procedure was applied to the final spectrum. ^1H–^{13}C COSY (HETCOR)[13] spectra were measured at 75.5 MHz with 8192 points and 800 scans per increment; 64 increments with zero filling to 128 points. The relaxation delay was 1 s and the polarization transfer delays were 3.9 and 1.95 ms, respectively.

WAXS diffractograms were obtained with a HZG/4A diffractometer; diffracted radiation was recorded by means of a proportional counter.

RESULTS AND DISCUSSION

Vibrational spectra of PNMLL

Figure 1 shows an infra-red spectrum of the amorphous PNMLL measured at room temperature immediately after casting from tetrahydrofuran solution, the spectra of PNMLL after 10 and 15 min and 7 days of crystallization on a KBr window, and a difference spectrum obtained by subtracting the spectrum of the amorphous component from the spectrum of the sample with the maximum degree of crystallinity. With time, many new bands appear and their intensities subsequently increase, whereas the intensities of other

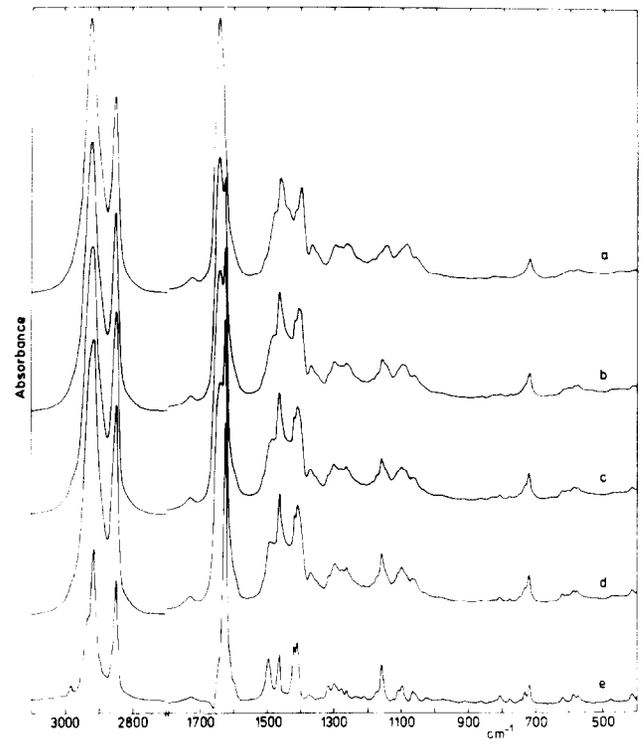

Figure 1 Infra-red spectra of PNMLL: (a) amorphous; crystallized for (b) 10 min; (c) 15 min; (d) 7 days; (e) difference spectrum of the crystalline phase

bands decrease. Following a time lag of some minutes after evaporation of the solvent from the sample or after melting the sample at 70°C, the ratio of the intensities A_{1628}/A_{1646} begins to increase with time; it reaches its maximum after about 1 week of crystallization. Far infra-red spectra of amorphous and of partly crystalline PNMLL are shown in *Figure 2*, Raman spectra of amorphous and of partly crystalline PNMLL and a difference Raman spectrum of the crystalline phase in *Figure 3*. Wavenumbers of the structurally important

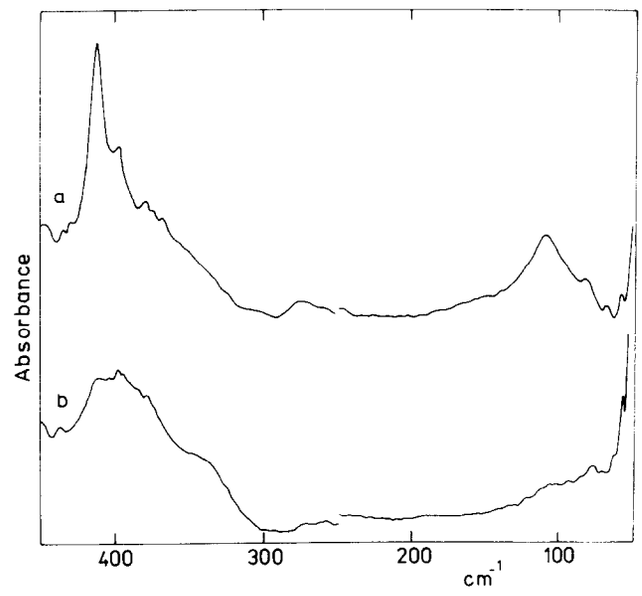

Figure 2 Far infra-red spectra of PNMLL: (a) partly crystalline; (b) amorphous

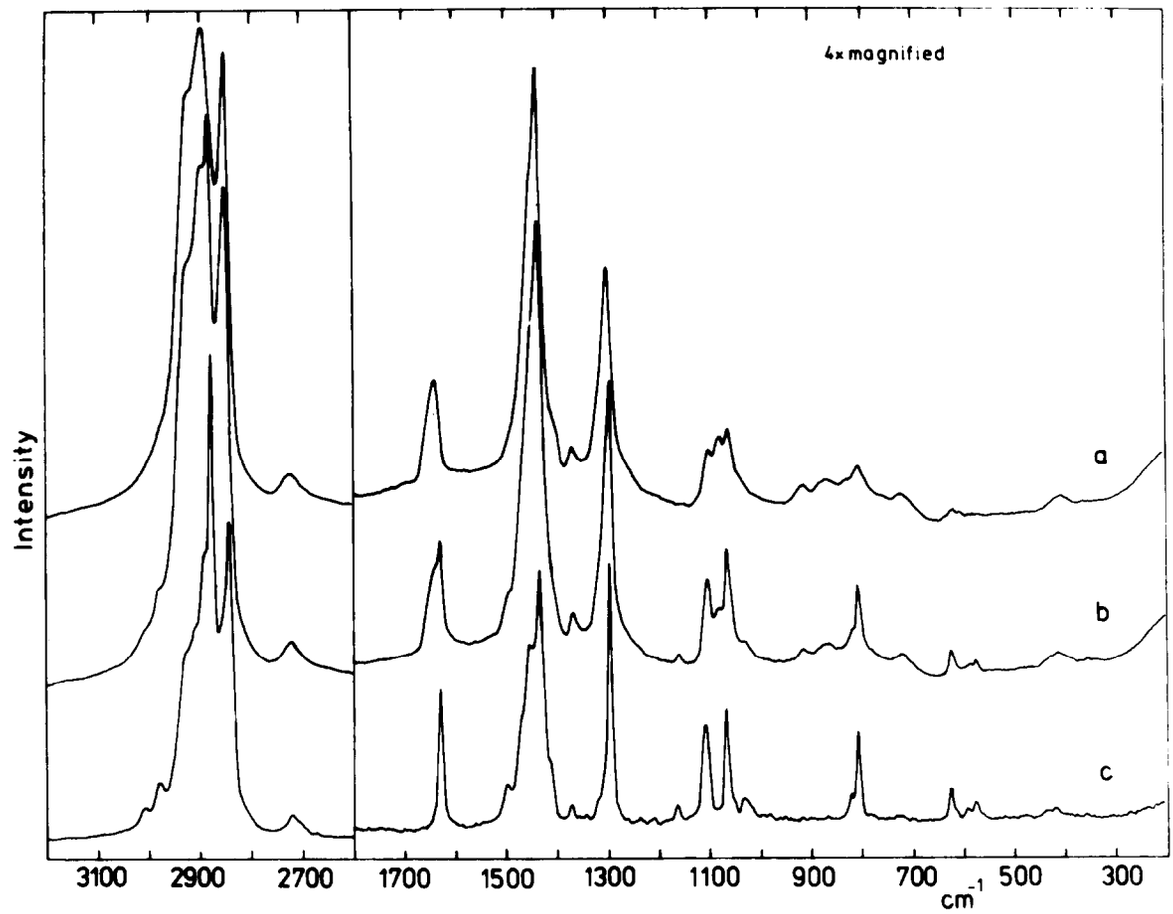

Figure 3 Raman spectra of PNMLL: (a) amorphous; (b) partly crystalline; (c) difference spectrum of the crystalline phase

vibrational bands of the amorphous and crystalline phases of PNMLL together with vibrational assignments[14–18] are summarized in *Table 1*.

Results of the infra-red dichroic measurement of PNMLL are demonstrated in *Figure 4*. It is seen that in particular the band at 1628 and also the band at 1646 cm^{-1} exhibit perpendicular infra-red dichroism with respect to the direction of film elongation. Also

Table 1 Main differences in the vibrational spectra of amorphous and crystalline PNMLL

Infra-red		Raman		
Amorphous	Crystalline	Amorphous	Crystalline	Assignment
	2982 w		2982 w	CH_2 str. asym.
2924 s			2925 sh	CH_2 str. asym.
	2914 vs	2919 sh		
		2895 vs		CH_3 str. sym.
			2880 s	
2852 s	2847 s	2849 s	2845 s	CH_2 str. sym.
1646 vs		1643 w		C=O str.
	1628 vs		1627 w	
1488 sh	1497 m		1496 w	CH_3 def. asym.
1465 m	1465 m		1465 sh	CH_2 sciss.
			1452 m	
1440 sh		1438 m		
1417 sh	1420 m			$CO-CH_2$ sciss.
1402 m	1412 m			CH_3 def. sym.
	1159 m			
		1102 w	1106 w	C–C str. of CH_2 *trans* sequences
		1079 w		
		1063 w	1064 w	
	380 w			skeletal deformation and amide torsion
360 w	260 w			
240 w	120 w			
80 w				

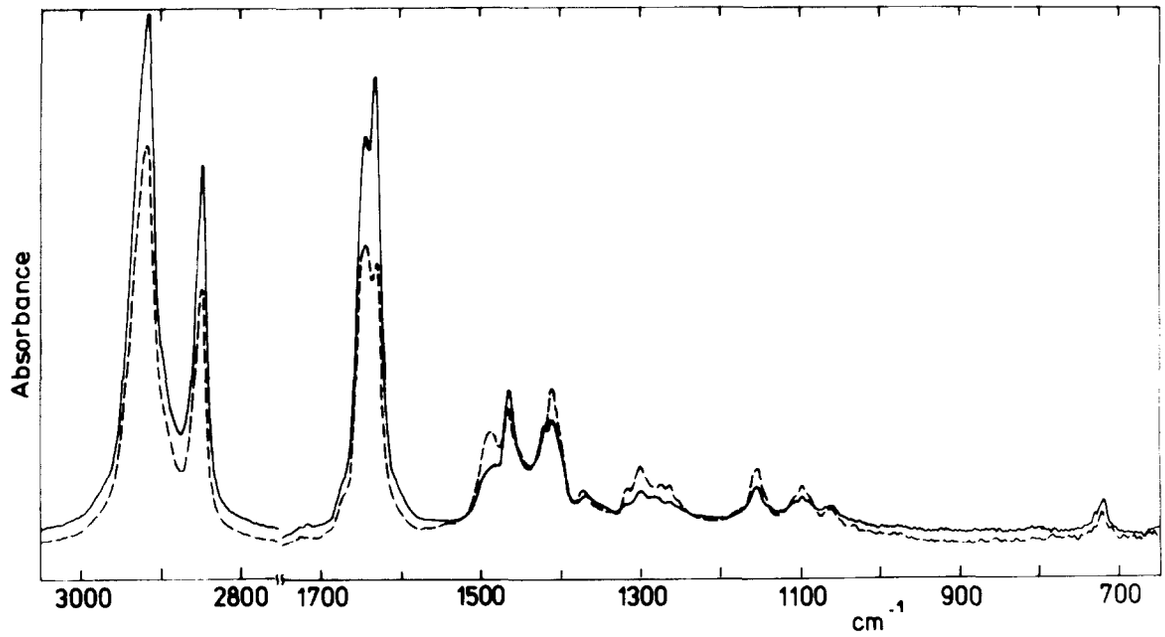

Figure 4 Infra-red spectra of oriented PNMLL; electric vector perpendicular (—) and parallel (···) to the direction of sample elongation

the bands in the region 3000–2800 cm^{-1} and some other bands are perpendicular. On the other hand, the absorption of the bands with a maximum at around 1492 cm^{-1}, the band at 1412 cm^{-1} and some other bands exhibit parallel dichroism.

Measuring the temperature dependence of the spectra of a 5% solution of PNMLL in $CHCl_3$, we have observed that with decreasing temperature the intensity of the band at 1485 cm^{-1} increases, and the wavenumber of the carbonyl band (at 1627 cm^{-1} at room temperature) is shifted to lower frequency values. The changes are continuous down to the temperature of $\sim -60°C$, where the solvent freezes. Two extreme solution spectra are shown in *Figure 5*.

As we also wanted to know more about the kinetics of the crystallization of PNMLL in the solid state, we have investigated, after melting of the partly crystalline sample, the rate of its recrystallization at lowered temperatures by means of Raman spectra. We found that above the temperature of $-50°C$, the major part of the sample is recrystallized within some tens of minutes. We were able to maintain the sample in the amorphous state for some hours by pouring it into a vessel with liquid nitrogen.

High-resolution n.m.r. spectra of PNMLL in solution

The ^1H n.m.r. spectrum of PNMLL measured at room temperature in TCE solution was assigned on the basis of a COSY spectrum, and the corresponding ^{13}C n.m.r. spectrum on the basis of the HETCOR spectrum shown in *Figure 6a*. In the ^{13}C n.m.r. spectrum the signals of most carbons occur in pairs, as well as the $N-CH_3$ and $N-CH_2$ signals in the ^1H n.m.r. spectrum. Evidently forms with both the *cis* and the *trans* orientation of the $N-CH_3$ group with respect to the carbonyl are present in comparable populations. The ^{13}C n.m.r. spectrum is very similar to the spectrum of *N*-methyllaurolactam (NMLL) studied previously by us as a model[19], and the pair components corresponding to carbons 2, 12 and $N-CH_3$ were assigned to the *cis* and *trans* forms in analogy to this model compound. The remaining line pairs were assigned from the HETCOR spectrum and the pair components from their line intensities. We see that at room temperature in TCE solution, the *cis* form

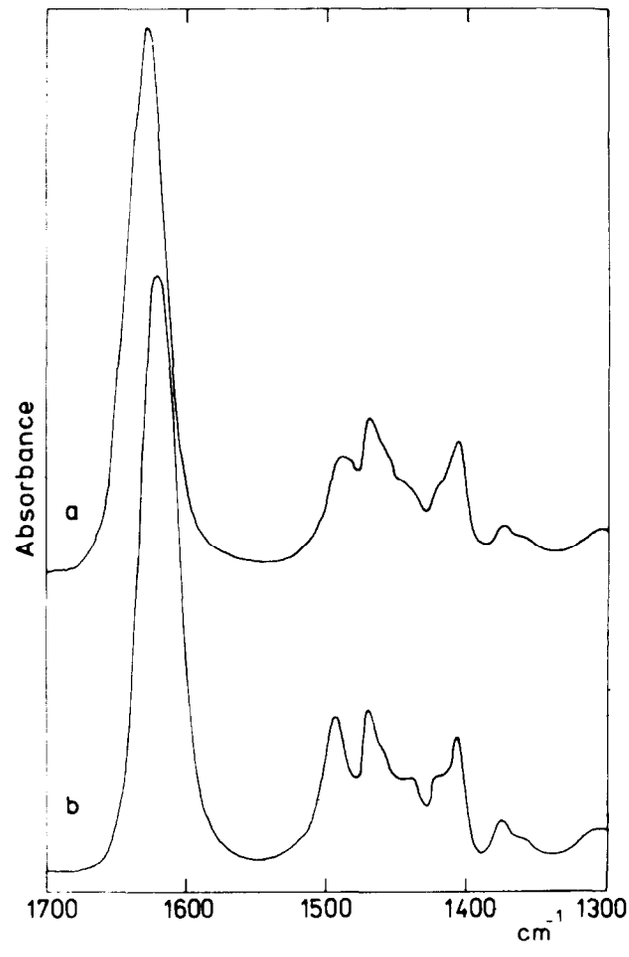

Figure 5 Infra-red spectra of 5% solution of PNMLL in $CHCl_3$ at different temperatures: (a) room temperature; (b) $t = -50°C$

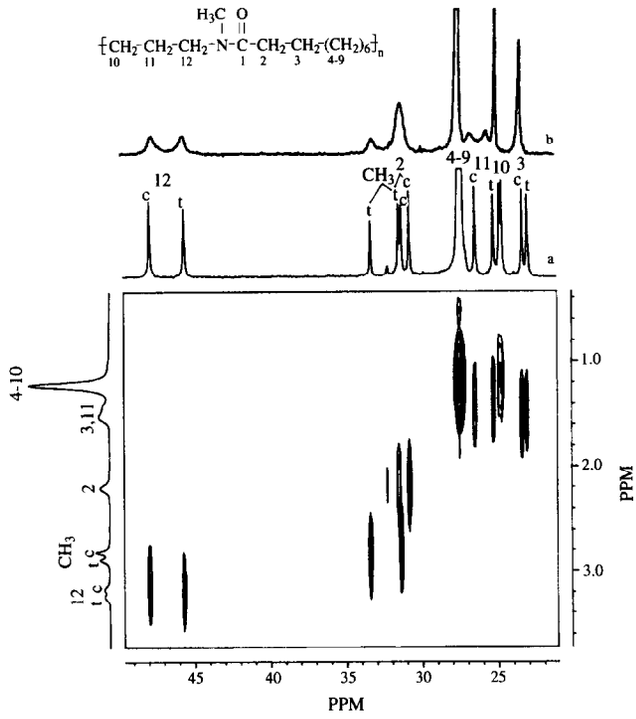

Figure 6 N.m.r. spectra of PNMLL in 1,1,2,2-tetrachloroethane-d_2 solution: (a) 2D ^1H–^{13}C HETCOR measured at 25°C; (b) 1D ^{13}C measured at 55°C

slightly predominates. The pair components of carbons 3 and 11 were assigned on the basis of their intensity relations.

With increasing temperature, the *cis–trans* line pairs in n.m.r. spectra gradually undergo exchange broadening and coalescence (*Figure 6b*), and the temperature dependence of the n.m.r. lineshapes can be used for the determination of the thermodynamic parameters of the *cis–trans* transition of PNMLL in solution. In a similar manner as in our previous communication[19], the experimental lineshapes of the ^{13}C signals of carbons 3, 11 and 12 were compared with those simulated by means of the relation[20]

$$S(\omega) = Im\{-iC\tau[2p_c p_t - \tau(p_c\alpha_t + p_t\alpha_c)]/ (p_c p_t - \tau^2\alpha_c\alpha_t)\} \quad (1)$$

where p_c, p_t are the populations of the *cis* and *trans* isomers and $\alpha_c = -[i(\omega_c - \omega) + 1/T_{2c} + p_t/\tau]$, with $p_c = p_t$ (this was considered permissible as in the studied temperature range the deviation of p_c/p_t from unity did not exceed ~5%) and $T_{2c} = T_{2t}$ chosen so that $1/\pi T_2$ varied from 0 for the doublet of C12 with $\Delta\nu = 170$ Hz to 2.5 s^{-1} for the doublet of C3 with $\Delta\nu = 25$ Hz. The result of this analysis in terms of the Eyring equation

$$\ln(kh/Tk_B) = -\Delta H^*_{ct}/RT + \Delta S^*_{ct}/R \quad (2)$$

where k_B and h are the Boltzmann and Planck constants, $k = 1/2\tau$ is the rate constant of isomerization, and the other symbols have their conventional meaning, is plotted in *Figure 7*. The points obtained from the three signal pairs can be fitted by a single straight line, yielding for the activation enthalpy $\Delta H^*_{ct} = 19.1$ kcal mol^{-1}, and for the activation entropy $\Delta S^*_{ct} = 5.6$ cal mol^{-1} K^{-1}.

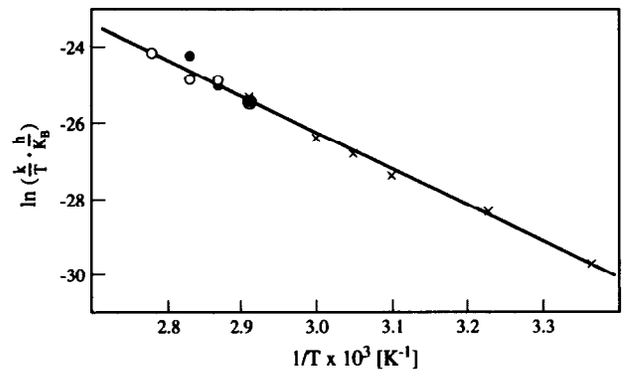

Figure 7 Temperature dependence of *cis–trans* isomerization of PNMLL in 1,1,2,2-tetrachloroethane-d_2 solution, plotted in terms of equation (2); k determined from lineshape of ^{13}C n.m.r. signals of carbons 3 (×), 11 (●) and 12 (○)

These values are very close to the values $\Delta H^*_{ct} = 19.5$ kcal mol^{-1} and $\Delta S_{ct} = 5.6$ cal mol^{-1} K^{-1} found by us for NMLL[19], thus corroborating the application of the latter as a model in the present study.

The results obtained from the n.m.r. spectra were correlated with *ab initio* and semiempirical AM1 quantum chemical calculations of the conformational properties of the *N*-methylated amide group in a model molecule CH_3–CH_2–N(CH_3)–CO–CH_3 (*Table 2*). All the calculations were performed using the GAMESS set of programs[21,22] running on a Silicon Graphics workstation Indy. A full optimization of all degrees of freedom was carried out using the gradient optimization routine in the program. The calculations were performed in C_1 symmetry. In order to obtain thermodynamic parameters that can be compared with experimental data obtained by spectroscopic measurements (ΔH), calculated *ab initio* energy differences ΔE were corrected by zero point vibrational energy and thermal corrections[23].

In comparison with experimental data, the *ab initio* calculated barrier to internal rotation around the N–CO bond is slightly lower; calculations were performed for the isolated single molecule whereas the experimental values were obtained for solution. The semiempirical AM1 value of the barrier is evidently underestimated. It is seen that the enthalpy difference between the *cis* and *trans* conformers is very small and this is in agreement with our findings that populations of the *cis* and *trans* forms of the *N*-methylated group in the solutions of NMLL[19] and PNMLL do not differ by more than 10% and 5%, respectively. The CH_3–CH_2N bond is approximately perpendicular to the plane of the *N*-methylated amide group for both *cis* and *trans* forms.

Table 2 Calculated (*ab initio* and AM1) barrier to internal rotation (kcal mol^{-1}) around the N–CO bond, enthalpy difference (kcal mol^{-1}) between the *cis* and *trans* conformers and torsional angles for CH_3–CH_2–N(CH_3)–CO–CH_3

	ΔH^*_{298}	ΔH^{ct}_{298}	ψ_c[a]	ψ_t[a]
6-31G	16.71	0.26	95.6	92.3
6-31G*	14.25	0.26	73.6	80.0
6-31 + G*	14.60	0.27	94.5	88.4
AM1	7.55	−0.02	83.9	100.3

[a] CH_3–CH_2–N(CH_3)–CO torsional angles (in degrees) for the *cis* and *trans* conformers, respectively

^{13}C solid-state n.m.r. spectra of PNMLL

PNMLL is typically semicrystalline at room temperature, thus the conventional ^{13}C CP/MAS/DD n.m.r. spectrum consists of a mixture of signals originating from the amorphous and crystalline phases. This situation is encountered in a number of other polymers. In non-methylated polyamides the signals of the two phases can be selectively recorded using the difference in their carbon spin lattice relaxation time (T_1^C)[24]. We have applied an analogous procedure to our system (see Experimental), even though we have not measured the respective T_1^C relaxation times; these can be different in PNMLL, particularly because of the presence of the usually rapidly rotating CH_3 group. Nevertheless, we believe that the inner consistency of our n.m.r. results (see below) together with the consistency with the results of other methods provide sufficient justification for the correctness of our approach.

The ^{13}C high-resolution solid-state spectra of PNMLL are given in *Figure 8a–c*. The spectra of the amorphous (*Figure 8c*) and crystalline (*Figure 8b*) phases show typical shapes often observed in other polymers; the 'amorphous' spectrum is broad and rather featureless, while the 'crystalline' spectrum consists of a number of sharp lines. The line of the NCH_2 carbon is broadened by residual dipolar interaction with ^{14}N; its lineshape is similar to that observed previously in the spectra of non-methylated polyamides[1,25] measured in an external field of 4.7 T. The conventional CP/MAS/DD spectrum shown in *Figure 8a* is obviously a weighted sum of these two spectra. Owing to the different efficiency of cross-polarization in the two phases, the signal of the amorphous phase in this spectrum is probably partially suppressed. The spectrum of the amorphous phase of PNMLL can be directly compared with the spectrum of PNMLL in solution presented in *Figure 8d* with an artificial broadening of 100 Hz. Both spectra are very similar to each other and thus an assignment of the solid-state spectrum was possible (*Figure 8c*). The large difference in the relative intensity of the central peak belonging to carbons 4–9 can be explained, for instance, by slightly differing chemical shifts of these carbons in the solid state. Based on the data obtained from solution measurements a tentative assignment of the peaks observed in the solid-state spectrum of the crystalline phase was also made (*Figure 8b*). The spectrum of the crystalline phase was interpreted assuming that only the *cis* form is present (see below).

The presence and position of the signal belonging to the CH_3 group in the spectra in *Figure 8* deserve closer attention, as the relaxation of the CH_3 group can be very fast due to its assumed rapid rotation (e.g. in solid PMMA at room temperature the T_1^C relaxation time of the α-methyl group carbon is of the order of 100 ms, while the T_1^C times of the other carbons are much longer[26]). The spectrum in *Figure 8b* shows the slowly relaxing part of the sample that is supposed to be the crystalline phase, while the spectrum in *Figure 8c* shows the rapidly relaxing part of the sample supposed to correspond to the amorphous phase. As the T_1^C relaxation of the methyl carbon can be substantially shorter than that of the other carbons, it may happen that in the spectrum of the crystalline phase no line belonging to the methyl group is present while in the

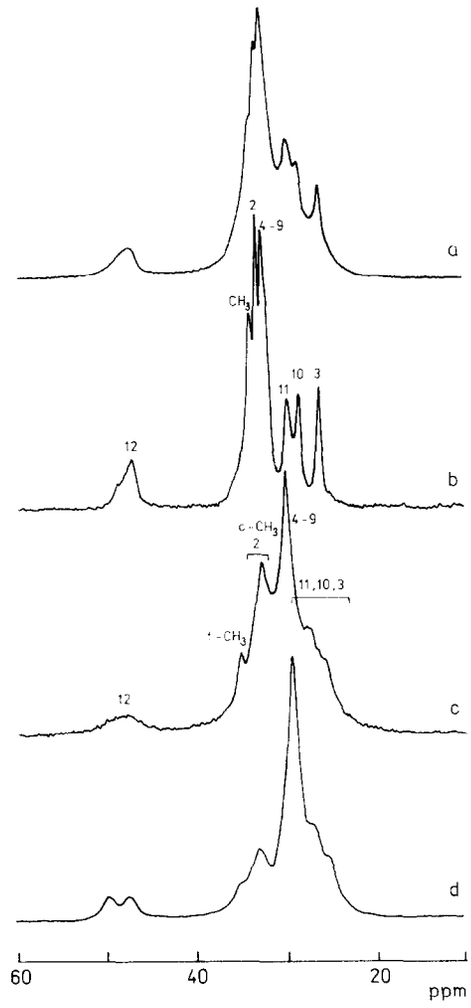

Figure 8 Aliphatic part of ^{13}C solid-state n.m.r. spectra of PNMLL: (a) conventional CP/MAS/DD spectrum; (b) spectrum measured with sequence for T_1^C measurements with cross-polarization with a delay of 10 s; (c) spectrum measured with single-pulse excitation with a relaxation delay of 1 s; (d) solution spectrum with 100 Hz line broadening. Numbering of atoms is the same as in *Figure 6*

spectrum of the amorphous phase the signals belonging to the methyl group originating from both phases can appear. To clarify this point, the so-called 'dipolar dephasing' experiment[27] was performed; the results are given in *Figure 9*. The dipolar dephasing experiment should select spectra showing peaks of carbons subjected to weak dipolar fields from surrounding protons, typically carbons with no directly bonded protons, carbons residing in highly mobile phases and carbons from rapidly rotating methyl groups. From *Figure 9* we can see that, as expected, the dipolar dephased spectrum (*Figure 9b*) is almost identical with the spectrum of the rapidly relaxing (amorphous) phase (*Figure 9a*), differing only by the presence of an additional peak at approx. 34 ppm. Similarly the spectrum of the slowly relaxing (crystalline) PNMLL component measured with an additional dipolar dephasing delay (*Figure 9c*) shows one peak at approx. 34 ppm. In both spectra, this peak can be assigned to the methyl group carbon in the crystalline phase (with long T_1^C relaxation time but weak dipolar interaction with protons), its position agreeing well with the solution data. Thus we may conclude that the spectra in *Figure 8b* and *c* truly

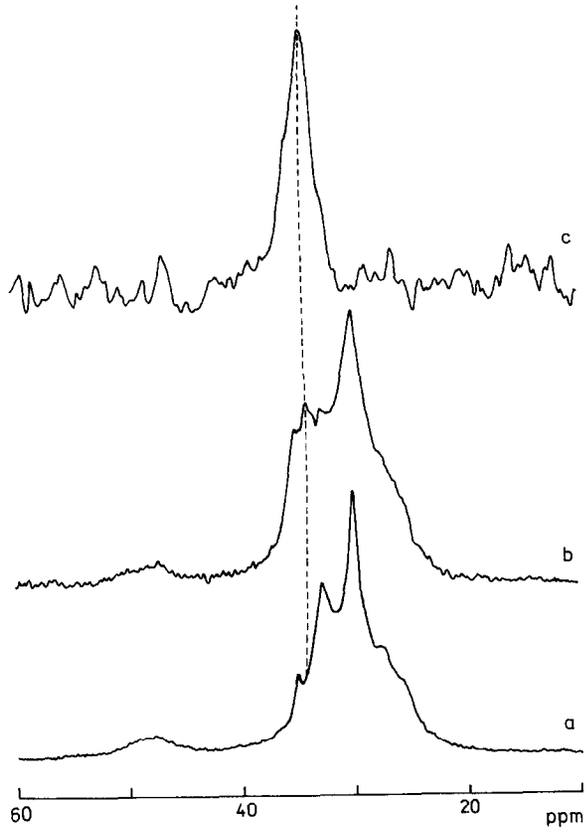

Figure 9 Aliphatic part of ^{13}C solid-state n.m.r. spectra of PNMLL measured with (a) single-pulse excitation with a relaxation delay of 1 s; (b) CP/MAS/DD with a dipolar dephasing delay of 40 μs; (c) sequence for T_1^C measurements with cross-polarization with a delay of 10 s and dipolar dephasing delay of 40 μs

represent the crystalline and amorphous phases, respectively.

Vibrational spectra of the PNMLL/PVPh blends

Vibrational spectra of pure PVPh were investigated recently[5]. Typical bands related to the vibrations of the phenyl group in PVPh are observed[18] at: 3330 cm^{-1} (i.r. O–H stretching), 1612, 1598 and 1512 cm^{-1} (i.r. and Raman C–C vibrations of the aromatic ring), 1233 and 1173 cm^{-1} (i.r. C–O stretching and C–H aromatic in-plane vibrations), and at 830 cm^{-1} (i.r.) and 840, 823 cm^{-1} (Raman) (C–H aromatic out-of-plane vibrations). The relevant parts of the spectra of PVPh are shown in *Figures 10e, 11a* and *12e*.

In the difference spectra of PNMLL in the blend with the molar concentration ratio PNMLL/PVPh 4:1 the intensity of the band at 1646 cm^{-1} is strongly diminished (*Figure 10b*). In the blends with the concentration ratios 1:1 and 1:4 the intensity of the band at 1628 cm^{-1} is also diminished and finally disappears and new bands at 1620 and 1590 cm^{-1} can be detected (*Figure 10c, d*). The shape of the difference spectrum in *Figure 10b–d* (1500–1530 cm^{-1}) indicates that the bands of PVPh in the spectra of the blends are also slightly changed as compared with the spectrum of pure PVPh. These changes could to some extent affect the shape of the difference spectra of PNMLL, nevertheless the main features of the spectra of the blends discussed above should be maintained. In the region 3700–3100 cm^{-1} the maximum of the broad band of PVPh is shifted from

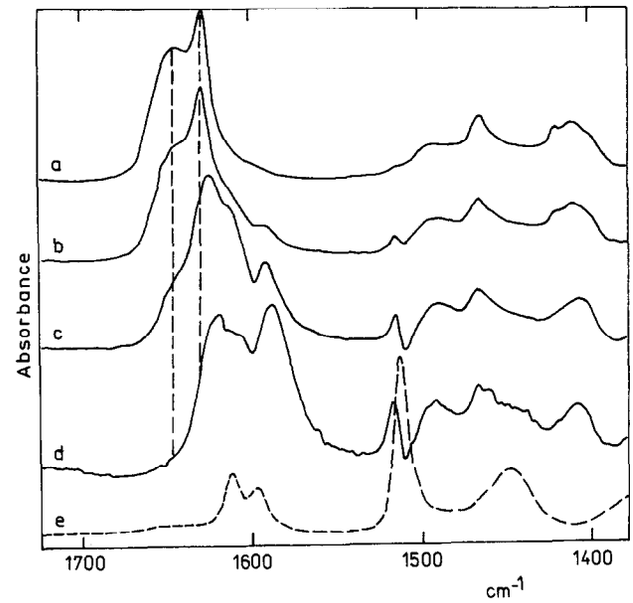

Figure 10 Comparison of infra-red spectra of semicrystalline PNMLL (a) and difference spectra of PNMLL in PNMLL/PVPh blends with the molar ratio 4:1 (b), 1:1 (c) and 1:4 (d). The spectrum of PVPh (e) is subtracted from the spectra of the blends

its original position at 3300 cm^{-1} in the pure PVPh to 3253 cm^{-1} in the blends with sufficient amount of PNMLL (*Figure 11*).

The PNMLL Raman bands of the PNMLL/PVPh blends (*Figure 12*) in the 1650–1580 cm^{-1} region show behaviour similar to that observed in the infra-red spectra, but the effects are less pronounced due to the lower relative intensity of the carbonyl bands with respect to the C–C stretching bands of the PVPh aromatic rings. The relative intensity of the doublet at 1105 and 1065 cm^{-1} decreases with increasing concentration of PVPh in the blends. The difference Raman spectra of PNMLL in PNMLL/PVPh blends 1:1 and 1:4 (*Figure 12c,d*) are similar to the Raman spectra of amorphous PNMLL (*Figure 3a*).

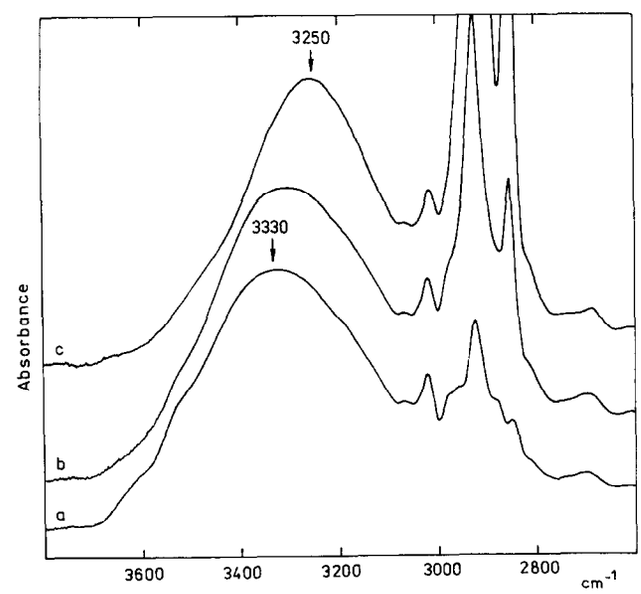

Figure 11 Influence of the hydrogen bonds. Infra-red spectrum of (a) PVPh; (b) PNMLL/PVPh blend 1:4; (c) PNMLL/PVPh blend 1:1

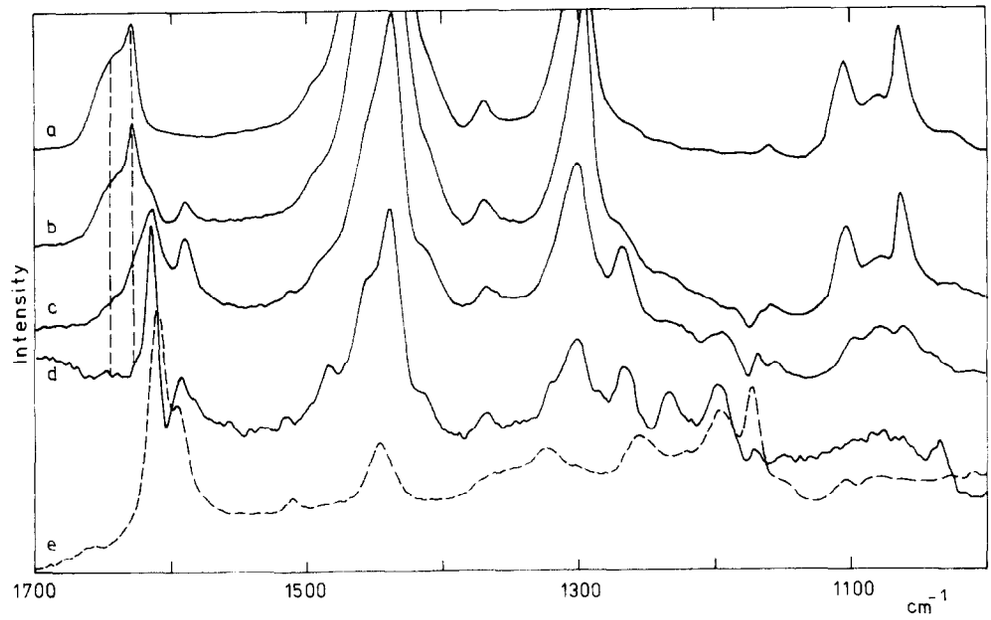

Figure 12 Comparison of Raman spectra of semicrystalline PNMLL (a) and difference spectra of PNMLL in PNMLL/PVPh blends with the molar ratio 4:1 (b), 1:1 (c) and 1:4 (d). The spectrum of PVPh (e) is subtracted from the spectra of the blends

^{13}C CP/MAS/DD n.m.r. spectra of PNMLL/PVPh blends and $T^{H}_{1\rho}$ relaxation time measurements

^{13}C CP/MAS/DD n.m.r. spectra of PNMLL, PVPh and PNMLL/PVPh blends are shown in *Figure 13*. The assignment of the ^{13}C n.m.r. spectrum of PVPh follows that of ref. 28. Comparison of the spectra of the blends and of pure PVPh and PNMLL indicates that the phenolic C–OH carbon peak of PVPh and C=O peak of PNMLL shift downfield on blending (*Table 3*). In the spectrum of the 4:1 blend two C=O peaks are clearly visible, one at a position corresponding to that in pure PNMLL, and the other shifted downfield by 1.6 ppm. Other carbon resonances of PVPh show only little change. In the aliphatic region the spectrum of the PNMLL/PVPh blend with the molar ratio 4:1 (*Figure 13b*) is very similar to the spectrum of pure PNMLL; this indicates the presence of the crystalline phase of PNMLL in the sample. On the other hand, in the spectra of the PNMLL/PVPh blends with the molar ratios 1:1 and 1:4 (*Figure 13c,d*), the shape of the PNMLL bands closely resembles the spectrum of amorphous PNMLL (*Figure 8c*) with slightly broadened peaks. In these blends the highest peak at 33 ppm characteristic of the crystalline PNMLL phase is replaced by the peak at 30 ppm assigned to the amorphous component. The peak in the spectrum of the 1:4 blend marked by an arrow is not an SSB, and we have not found an explanation for its presence.

In heterogeneous systems the measurement of proton relaxation can provide information about the intimacy of the mixing. We measured $T^{H}_{1\rho}$ relaxation times in the PNMLL/PVPh blends and also in the pure components. The results are summarized in *Table 3*. The $T^{H}_{1\rho}$ relaxation times given in *Table 3* were determined as average values from all detected PNMLL or PVPh ^{13}C peaks. We observed a single exponential decay of the proton magnetization for the PVPh signals in all samples and for the PNMLL signals in the PNMLL/PVPh blends of the molar ratios 1:4 and 1:1. For pure PNMLL and the PNMLL/PVPh blend 4:1 a single exponential behaviour was observed only with some peaks (C=O, N–CH_2) while with other CH_2 peaks a non-exponential decay was observed. This non-exponential decay could be well fitted assuming two relaxation times with the shorter component approximately equal to 1 ms and with

Figure 13 ^{13}C CP/MAS/DD n.m.r. spectra of (a) PNMLL; (b) PNMLL/PVPh 4:1 (c) PNMLL/PVPh 1:1; (d) PNMLL/PVPh 1:4; (e) PVPh. SSB denotes spinning sidebands

Table 3 ^{13}C chemical shifts and relaxation times $T_{1\rho}^{H}$ of PNMLL/PVPh blends

PNMLL/PVPh (molar ratio)	X-ray crystallinity	^{13}C chem. shift (ppm)		$T_{1\rho}^{H}$ (ms)	
		C=O	C–OH	PNMLL	PVPh
1:0	0.28	170.7	–	11.0	
4:1	0.28	170.6[a]; 172.2[a]	155.7	11.0	–[b]
1:1	0	173.9	155.6	3.2	3.3
1:4	0	175.5	154.2	5.0	5.1
0:1	0	–	152.8	–	6.6

[a] Two peaks were observed (see text)
[b] Not determined due to low signal-to-noise ratio of the PVPh bands

the longer component in the ranges 9.8–12.5 ms (pure PNMLL) and 8.4–14.0 ms (the PNMLL/PVPh blend 4:1). As the value of the longer component was very close to the value of fitted $T_{1\rho}^{H}$ for the exponentially decaying peaks, it was used in the evaluation of the average $T_{1\rho}^{H}$ value in *Table 3*.

Structure of PNMLL

According to our n.m.r. results, in solution there exists an equilibrium between the *cis* and *trans* conformation of the amide group. Near room temperature, the population ratio of both conformations is approximately 1:1. With decreasing temperature the amount of the *cis* conformation is increasing; above −40°C the equilibrium is established at an observable rate (at 233 K, $k = 8.2 \times 10^{-5}\,s^{-1}$).

Depending on the molecular weight and on sample preparation, PNMLL in the solid state contains 0–40% of the crystalline phase, the rest being amorphous[7]. Both in the vibrational and in the solid-state n.m.r. spectra, two systems of bands are expected to appear, corresponding to the presence of the *cis* and *trans* conformations in the amorphous phase. On the other hand, bands corresponding to only one of the possible amide conformations can be expected for the crystalline phase.

In general, it can be stated that the vibrational spectra of the amorphous samples exhibit broader bands than the spectra of the crystalline phase. This corresponds to the lower conformational regularity in the amorphous phase. A conspicuous difference in the vibrational spectra of amorphous and crystalline PNMLL appears in the vibration of the amide carbonyl: in the amorphous phase, a broader band can be found at 1648 cm^{-1}. A similar band is observed also in the spectra of PNMLL solutions. In view of the n.m.r. results, this infra-red band at 1648 cm^{-1} corresponds to both the *cis* and the *trans* structures of the *N*-methylated amide group. In the course of the crystallization of solid PNMLL at room temperature, a new narrow amide carbonyl band begins to develop very quickly at 1628 cm^{-1}, corresponding to the crystalline phase. We think that the shift of the carbonyl band in the spectrum of crystalline PNMLL to the lower wavenumber in the crystalline phase is caused by intermolecular forces in the crystal lattice, not by a change in the populations of the *cis* and *trans* forms in the *N*-methylated amide groups, as supposed in ref. 7.

Analysis of the infra-red dichroism of the bands in the oriented PNMLL film has shown that the polymer chains are oriented in the direction of sample elongation. From the opposite dichroism of the bands of the stretching vibration of the amide carbonyl and of the symmetric deformation of the CH_3 group it follows that the transition dipole moments of these two vibrations are mutually perpendicular. Integration of the area of the carbonyl bands has shown that the orientation of the crystalline part of PNMLL is higher than the orientation of the amorphous part. Such dichroic behaviour can be explained by assuming that in the crystalline phase of PNMLL the *N*-methyl groups assume *cis* orientation with respect to the carbonyl oxygens.

In the infra-red spectrum, the band of the $CO–CH_2$ scissoring vibration is apparent only in the crystalline phase at 1420 cm^{-1} (*Figure 1b*). A similar increase in intensity for such a band has been found with poly(ε-caprolactam) in the planar conformation and assigned to the scissoring vibration of the CH_2 group, for which the dipole moment change is coplanar with that of the stretching vibration of the vicinal C=O group[15]. From this we have concluded that in the crystalline phase of PNMLL also the $CH_2–CH_2$ bond vicinal to the carbonyl lies in the *trans* position with respect to the C–N amide bond.

The Raman bands 1050–1120 cm^{-1} were assigned to the C–C stretching vibrations in the CH_2 sequences[16]. In comparison with amorphous PNMLL, the spectrum of partly crystalline PNMLL exhibits higher relative intensity of the bands in the doublet at 1064 and 1105 cm^{-1} with respect to the band at 1079 cm^{-1}. After having subtracted the spectrum of the amorphous PNMLL from the spectrum of partly crystalline PNMLL, the band at 1079 cm^{-1} completely disappears. Using the results of the spectroscopic analysis of conformationally disordered n-alkanes[17], we can correlate the intensities of the 1064 and 1105 cm^{-1} bands with the concentration of long CH_2 sequences having the *trans* planar conformation in the PNMLL samples.

Measuring the temperature dependences of the spectra of a solution of PNMLL in $CHCl_3$ we have observed great intensity changes of the band near 1490 cm^{-1} between −20 and −50°C. Similar behaviour of the infra-red bands was found in the spectra of NMLL[19] and we have shown that in the spectra of solid PNMLL these changes continue down to −150°C; similar behaviour can be even better observed with amorphous poly(*N*-methyl caprylolactam)[29]. According to n.m.r. results, at these temperatures a *cis–trans* conformational transition about the *N*-methylated amide bond is so slow that it practically cannot be observed below −50°C. We conclude that the increase in the infra-red absorption near 1490 cm^{-1} with decreasing temperature is not the result of a conformational change, but could be caused either by a change in the electro-optical parameters of the molecules, or by temperature changes of methyl group rotation about the $N–CH_3$ bond. The observed intensity changes are fully analogous to those found with the asymmetric deformation of $O–CH_3$ groups in poly(methyl methacrylate)[30], which we have explained by relaxation changes caused by rotation about the $O–CH_3$ bond. Therefore we think that also in the case of PNMLL the intensity of the CH_3 asymmetric deformation band is determined by a temperature-dependent relaxation mechanism.

From the solid-state n.m.r. spectra we can see that the amorphous phase (*Figure 8c*) shows a clear peak at about 35 ppm assigned, by comparison with solution data, to

the CH_3 carbon in the *trans* form. A similar peak in the spectrum of the crystalline phase (*Figure 8b*) is missing. The peaks in the spectrum of the crystalline phase can be interpreted very well assuming the presence of only the *cis* form. This is in agreement with the infra-red results. On the other hand, the *cis* NCH_2 peak should be found more downfield according to the solution data. According to our assignment shown in *Figure 8*, the peak of carbons 4–9 in the spectrum of the crystalline phase is shifted downfield by 2.8 ppm in comparison with the spectrum of the amorphous phase. In view of the *γ-gauche* effect[10], both the direction and size of this shift are in agreement with the presence of long CH_2 sequences in mutual *trans* orientation in the crystalline phase, as found from vibrational spectra.

Structure and interactions in PNMLL/PVPh blends

Strong interactions between the PNMLL and PVPh chains in the PNMLL/PVPh blends are manifested in the infra-red spectra by the intensity decrease of the band at 1648 cm^{-1} and in the blends with higher concentration of PVPh also by the decrease of the crystalline band at 1628 cm^{-1} (*Figure 11*). New carbonyl bands are detected at 1620 and 1590 cm^{-1}. As both bands occur in the spectra of 1:1 and 1:4 PNMLL/PVPh blends where no crystalline phase exists according to the X-ray and n.m.r. measurements, they must originate from the amorphous PNMLL intimately mixed with PVPh; we suppose that the band at the lower frequency (1590 cm^{-1}) corresponds to carbonyl groups hydrogen-bonded with PVPh. The formation of strong hydrogen bonds between the C=O groups of PNMLL and O–H groups of PVPh is also proved by the shift of the O–H stretching band to lower frequency (by ~80 cm^{-1}) in the PNMLL blends with sufficient amount of PVPh (*Figure 12*). The direction of this shift shows that the hydrogen bonds between the C=O and O–H groups in the blends are stronger than the hydrogen bonds in pure PVPh[31].

The intensity decrease of the doublet at 1064 and 1105 cm^{-1} in the Raman spectra of the PNMLL/PVPh blends (*Figure 13*) indicates that the population of the CH_2 *trans* sequences, typically present in the crystalline component of PNMLL, is greatly diminished in the PNMLL/PVPh blends.

In the ^{13}C CP/MAS/DD n.m.r. spectra of PNMLL/PVPh blends (*Figure 13*) the downfield shifts of the C–OH and C=O resonances are indicative of the intermolecular hydrogen-bonding interactions between PNMLL and PVPh. In the 4:1 PNMLL/PVPh blend the crystalline phase of PNMLL is present, while the 1:1 and 1:4 PNMLL/PVPh blends are completely amorphous. This is in agreement with the results of the infra-red and Raman measurements. The two phases present in the 4:1 blend are also manifested by the two C=O peaks observed in the ^{13}C CP/MAS/DD n.m.r. spectrum of this blend (*Figure 13b*). One peak can be assigned to the non-interacting (crystalline) PNMLL and the other one to the amorphous PNMLL forming hydrogen bonds with PVPh. The broadening of PNMLL peaks in blends as compared with the spectra of pure PNMLL can probably be related to the formation of hydrogen bonds in the blends.

In the $T_{1\rho}^H$ relaxation time measurements, only some of the PNMLL peaks showed non-exponential character, and the relative weights of the two fitted $T_{1\rho}^H$ components obtained for different peaks were not consistent. This suggests that the non-exponential behaviour does not directly reflect the phase structure of PNMLL. Nevertheless, this non-exponential behaviour is probably in some way related to the existence of the crystalline phase, as it was observed only with the samples containing non-negligible amounts of the crystalline phase. For the 1:4 and 1:1 PNMLL/PVPh blends, the $T_{1\rho}^H$ relaxation times of PNMLL and PVPh are the same within experimental error; this means that fast proton spin diffusion occurs among all protons. The intimacy of mixing can be estimated using the formula for the maximum diffusive path length[32], $L = (6DT_{1\rho}^H)^{1/2}$. With $T_{1\rho}^H = 5 \times 10^{-3}$ s and $D = 8 \times 10^{-16}$ m^2 s^{-1} (a value recently found in rigid poly(methyl methacrylate)/polystyrene copolymers[33]), and taking into account that in the on-resonance $T_{1\rho}^H$ experiment the spin-diffusion coefficient D is scaled[34] by a factor of 1/2, we obtained $L \sim 3.5$ nm. We may expect that the value of the spin-diffusion coefficient D in our system is lower than 8×10^{-16} m^2 s^{-1} as amorphous PNMLL is well above T_g at room temperature. Thus we may conclude that PNMLL and PVPh are intimately mixed on a scale <3 nm. *Table 3* shows that the $T_{1\rho}^H$ relaxation times of the PNMLL/PVPh blends of the molar ratios 1:4 and 1:1 are shorter than those of pure PNMLL and PVPh; this indicates that the change in the relaxation time on blending is caused not only by averaging due to fast spin diffusion but also by changes of the structure affected by hydrogen-bonding interactions.

CONCLUSIONS

1. In PNMLL, there exists an equilibrium between the *cis* and *trans* conformations of the methylated amide group and both forms can be detected in solution by high-resolution n.m.r. spectra. The presence of both conformations of the amide bond is also reflected in the solid-state ^{13}C n.m.r. spectra of the amorphous phase of PNMLL. Contrary to previous reports[7], the measurement of the infra-red dichroism of the oriented film shows that in the crystalline phase the methyl group assumes *cis* orientation with respect to the carbonyl oxygen. This is in accord with the absence of the CH_3 peak of the *trans* form in the solid-state n.m.r. spectrum of the crystalline phase. According to Raman and infra-red spectra, and in agreement with solid-state n.m.r. spectra of the crystalline phase of PNMLL, long CH_2 sequences in mutual *trans* positions and in *trans* position with respect to the CO–N(CH_3) bond of the amide group are present in the crystalline phase of PNMLL.
2. In the PNMLL/PVPh blends, significant shifts of some bands in both the vibrational and n.m.r. spectra confirm the expected strong hydrogen-bonding interactions which are evidently connected with further observed structural changes: crystallinity diminishing with increasing PVPh content and a concurrent decrease in the content of long CH_2 *trans* sequences in the aliphatic chain. $T_{1\rho}^H$ measurements reveal intimate mixing of the components on a scale <3 nm, considerably smaller than in the previously studied cases of non-interacting and weakly interacting polymers[1,2]. Moreover, the $T_{1\rho}^H$ value observed in these intimately mixed blends is lower than that of

either of the two components; this was not observed in the two previously studied types of blends, and it is evidently connected with deeper structural changes in the presently studied materials.

ACKNOWLEDGEMENTS

This study was supported by Grant 45040 of the Grant Agency of the Academy of Sciences of the Czech Republic and by Grant 106/94/1688 of the Grant Agency of the Czech Republic. The authors wish to thank Dr J. Baldrian for the X-ray diffraction measurements.

REFERENCES

1 Schmidt, P., Dybal, J., Straka, J. and Schneider, B. *Makromol. Chem.* 1993, **194**, 1757
2 Straka, J., Schmidt, P., Dybal, J., Schneider, B. and Spěváček, J. *Polymer* 1995, **36**, 1147
3 Qin, Ch., Pires, A. T. N. and Belfiore, L. A. *Macromolecules* 1991, **24**, 666
4 Painter, P. C., Tang, W., Graf, J. F., Thomson, B. and Coleman, M. M. *Macromolecules* 1991, **24**, 4310
5 Serman, C. J., Painter, P. C. and Coleman, M. M. *Polymer* 1991, **32**, 1049
6 Li, D. and Brisson, J. *Polymer* 1994, **35**, 2078
7 Shalaby, S. W., Fredericks, R. J. and Pearce, E. M. *J. Polym. Sci., Polym. Phys. Edn* 1974, **12**, 223
8 Puffr, R., Tuzar, Z., Mrkvičková, L. and Šebenda, J. *Makromol. Chem.* 1983, **184**, 1957
9 Puffr, R. and Šebenda, J. *Makromol. Chem., Macromol. Symp.* 1986, **3**, 249
10 Komoroski, R. C. (Ed.) 'High Resolution NMR Spectroscopy of Synthetic Polymers in Bulk', VCH Publishers, Deerfield Beach, FL, 1986
11 Torchia, D. A. *J. Magn. Reson.* 1978, **30**, 613
12 Nagayama, K., Kumar, A., Wuthrich, K. and Ernst, R. R. *J. Magn. Reson.* 1980, **40**, 321
13 Bax, A. and Morris, G. *J. Magn. Reson.* 1981, **42**, 501
14 Jakeš, J. and Krimm, S. *Spectrochim. Acta* 1971, **27A**, 19
15 Schmidt, P. and Schneider, B. *Collect. Czech. Chem. Commun.* 1963, **28**, 2685
16 Snyder, R. G. *J. Chem. Phys.* 1967, **47**, 1316
17 Zerbi, G., Magni, R., Gussoni, M., Holland Moritz, K., Bigotto, A. and Dirlikov, S. *J. Chem. Phys.* 1981, **75**, 3175
18 Socrates, G., 'Infrared Characteristic Group Frequencies', John Wiley, New York, 1980
19 Doskočilová, D., Dybal, J. Schmidt, P., Schneider, B. and Kříž, J. *J. Mol. Struct.* 1995, **350**, 9
20 Binsch, G. in: 'Dynamic NMR Spectroscopy' (Eds L. M. Jackman and F. A. Cotton), Academic Press, New York, 1975, p. 49
21 Dupuis, M., Spangler, D. and Wendolski, J. J. 'NRCC Software Catalog', 1980, p. 1 (Program QC01)
22 Schmidt, M. W., Baldridge, K. K., Boatz, J. A., Jensen, J. H., Koseki, S., Gordon, M. S. *et al. QCPE Bull.* **10**, 52
23 Allinger, N. L., Grev, R. S., Yates, B. F. and Schaefer III, H. F. *J. Am. Chem. Soc.* 1990, **112**, 114
24 Hatfield, G. R., Glans, J. H. and Hammond, W. B. *Macromolecules* 1990, **23**, 1654
25 Spěváček, J., Straka, J. and Schneider, B. *J. Appl. Polym. Sci.: Appl. Polym. Symp.* 1991, **48**, 371
26 Gabrys, B., Horii, F. and Kitamaru, R. *Macromolecules* 1987, **20**, 175
27 Opella, S. J. and Frey, M. H. *J. Am. Chem. Soc.* 1979, **101**, 5854
28 Zhang, X., Takegoshi, K. and Hikichi, K. *Macromolecules* 1991, **24**, 5756
29 Schneider, B. *et al. Collect. Czech. Chem. Commun.* in press
30 Schmidt, P., Schneider, B., Dirlikov, S. and Mihailov, M. *Eur. Polym. J.* 1975, **11**, 229
31 French, R. N., Machado, J. M. and Lin-Vien, D. *Polymer* 1992, **33**, 755
32 McBrierty, V. J., Douglass, D. C. and Kwei, T. K. *Macromolecules* 1978, **11**, 1265
33 Clauss, J., Schmidt-Rohr, K. and Spiess, H. W. *Acta Polym.* 1993, **1**, 44
34 Henrichs, P. M., Tribone, J., Massa, D. J. and Hewitt, J. M. *Macromolecules* 1988, **21**, 1982